Revista ALCONPAT
www.revistaalconpat.org
eISSN 2007-6835
Revista de la Asociación Latinoamericana de Control de Calidad, Patología y Recuperación de la Construcción

Alkali-activated cements based on limestone-fly ash: Effect of the MgO-NaOH activation, compressive strength and reaction products

I. E. Betancourt-Castillo[1], O. Burciaga-Díaz[2]*
*Contact author: oswaldo.bd@saltillo.tecnm.mx
DOI: https://doi.org/10.21041/ra.v14i2.737

Received: 25/04/2024 | Received in revised form: 12/05/2024 | Accepted: 14/05/2024 | Published: 15/05/2024

ABSTRACT

This study investigates the effects of alkaline activation with MgO-NaOH on the compressive strength and reaction products of alkali activated cements of limestone powder (PClz) and Class C fly ash (CV). Results showed that substitutions of 25%<PClz<75% allowed 25-76 MPa at 360 days of curing, obtaining the highest strength with 25%PClz-75%CV and 50%PClz-50%CV with 10 and 12% NaOH-MgO, respectively. The results suggest that PCLz participates in hydration reactions as a filler and nucleating agent while the CV is the main contributor to the advance of the chemical reactions. X-ray diffraction (XRD), Thermal analysis (TA) and Scanning Electron Microscopy (SEM) indicated the formation of M-S-H, and C, N-A-S-H-type products, in addition to carbonate phases such as hydrotalcite, gaylussite, and pirssonite. Traces of unreacted MgO were not observed indicating its whole incorporation into the reaction products.

Keywords: alkali-activated cements; limestone powder; fly ash; alkaline-activation; mechanical properties; microstructural characterization.

Cite as: Betancourt-Castillo, I. E., Burciaga-Díaz, O. (2024), "*Alkali-activated cements based on limestone-fly ash: Effect of the MgO-NaOH activation, compressive strength and reaction products*", Revista ALCONPAT, 14 (2), pp. 141 – 156, DOI: https://doi.org/10.21041/ra.v14i2.737

[1] División de Estudios de Posgrado e Investigación, Tecnológico Nacional de México/I.T. de Saltillo, Saltillo, Coahuila, México.

Contribution of each author
In this study the author I.E. Betancourt-Castillo contributed with the first original draft, research, data recopilation, formal analysis of the results, interpretation and discussion of the results; the author O. Burciaga-Díaz with the original idea, review and editing of the article, conceptualization, supervision of the project and gathering funds

Discussions and subsequent corrections to the publication
Any dispute, including the replies of the authors, will be published in the first issue of 2025 provided that the information is received before the closing of the third issue of 2024.

Cementos activados alcalinamente basados en piedra caliza-ceniza volante: Efecto de la activación con MgO-NaOH, resistencia a la compresión y productos de reacción

RESUMEN

Este estudio investiga los efectos de la activación alcalina con MgO-NaOH sobre la resistencia a la compresión y los productos de reacción de los cementos activados alcalinamente con polvo de piedra caliza (PClz) y ceniza volante de Clase C (CV). Los resultados mostraron que las sustituciones de 25%<PClz<75% permitieron 25-76 MPa a los 360 días de curado, obteniendo la mayor resistencia con 25%PClz-75%CV y 50%PClz-50%CV con 10 y 12% NaOH-MgO respectivamente. Los resultados sugieren que el PCLz participa en las reacciones de hidratación como agente de relleno y nucleante mientras que el CV es el principal contribuyente al avance de las reacciones químicas. La difracción de rayos X (XRD), el análisis térmico (TA) y microscopía electrónica de barrido (SEM) indicaron la formación de productos del tipo M-S-H y C, N-A-S-H, además de fases carbonatadas como hidrotalcita, gaylussita y pirssonita. No se observaron trazas de MgO sin reaccionar, lo que indica su completa incorporación en los productos de reacción.

Palabras clave: Cementos activados alcalinamente; polvo de caliza; ceniza volante; activación alcalina; propiedades mecánicas; caracterización microestructural.

Cimentos ativados alcalinamente à base de calcário-cinzas volantes: Efeito da ativação com MgO-NaOH, resistência à compressão e produtos de reação

RESUMO

Este estudo investiga os efeitos da ativação alcalina com MgO-NaOH na resistência à compressão e nos produtos de reação dos cimentos ativados alcalinamente com pó de calcário (PClz) e cinzas volantes de Classe C (CV). Os resultados mostraram que substituições de 25% < PClz < 75% permitiram resistências à compressão de 25-76 MPa aos 360 dias de cura, obtendo a maior resistência com 25% PClz-75% CV e 50% PClz-50% CV com 10 e 12% NaOH-MgO respectivamente. Os resultados sugerem que o PCLz participa das reações de hidratação como agente de enchimento e nucleante, enquanto o CV é o principal contribuinte para o avanço das reações químicas. A difração de raios-X (XRD), análise térmica (TA) e microscopia eletrônica de barredura (SEM) indicaram a formação de produtos do tipo M-S-H e C, N-A-S-H, além de fases carbonatadas como hidrotalcita, gáilussita e pirssonita. Vestígios de MgO não reagido não foram observados, indicando sua completa incorporação nos produtos de reação.

Palavras-chave: Cimentos ativados alcalinamente; pó de calcário; cinza volante; ativação alcalina; propriedades mecânicas; caracterização microestrutural.

Legal Information

Revista ALCONPAT is a quarterly publication by the Asociación Latinoamericana de Control de Calidad, Patología y Recuperación de la Construcción, Internacional, A.C., Km. 6 antigua carretera a Progreso, Mérida, Yucatán, 97310, Tel.5219997385893, alconpat.int@gmail.com, Website: www.alconpat.org

Reservation of rights for exclusive use No.04-2013-011717330300-203, and ISSN 2007-6835, both granted by the Instituto Nacional de Derecho de Autor. Responsible editor: Pedro Castro Borges, Ph.D. Responsible for the last update of this issue, ALCONPAT Informatics Unit, Elizabeth Sabido Maldonado.

The views of the authors do not necessarily reflect the position of the editor.

1. INTRODUCTION

The cement industry is currently undergoing a significant transformation, driven by a collective effort to embrace sustainable practices and reduce environmental impact. This shift entails a multidisciplinary approach aimed at promoting the reuse of waste materials, implementing low carbon footprint technologies, optimizing material design for efficiency, and reducing the clinker factor, as a primary component of traditional cement production (Villagrán-Zaccardi et al. 2022).
A notable advancement is the development of alkali activated cements, which incorporate materials like pulverized limestone and other alternatives as the industrial by-products. These cements have emerged as a more sustainable alternative to Portland cement, offering numerous advantages across various facets of sustainability. They have been shown to reduce costs, lower production energy requirements, decrease CO_2 emissions, and contribute to circular economy goals through efficient design principles (Alsalman et al. 2021; Mendoza-Rangel et al. 2023). Additionally, alkali activated cements exhibit favorable mechanical and durability properties, further enhancing their consideration as sustainable construction materials.
Of particular interest is the use of by-products such as fly ash to enhance the sustainability of these cementitious materials (Mohamed et al. 2023). This approach not only helps to minimize waste but also underscores the industry's commitment to maximizing resource efficiency and minimizing environmental impact (Juenger et al., 2019).
Limestone is a naturally abundant mineral with high crystallinity and fly ash (CV) is an industrial by-product derived from the burning of mineral coal in energy powder plants with a yearly production of approximately 750 million tons and 80% of it is disposed on landfills (Temujin et al. 2019). These materials offer interesting properties and are a viable alternative to traditional Portland cement by reducing the carbon emissions associated with the clinker production (R.M. Andrew, 2018). Limestone is commonly used for producing Portland cement, however in recent years it has gained interest as a cementitious precursor in alkali activated cements (Chan and Zhang et al. 2023). Its use in blended cements seems to be promissory as they can exhibit improved durability and long-term performance, making them attractive for a variety of construction applications; however more investigation is necessary (Hosam M. Saleh and Samir B. Eskander, 2020; Díaz-Aguilera, 2024).
The alkaline activation of blended cements using a combination of magnesium oxide (MgO) and sodium hydroxide (NaOH) has been little explored as a promising strategy to enhance the reactivity and performance of these raw materials. Alkaline activation involves the dissolution and recombination of amorphous phases contained in fly ash leading to the consolidation of stable cementitious products. Both processes result in the precipitation of C,N-A-S-H-type gels and other secondary phases which contribute to the strength and durability (O. Burciaga-Díaz *et al.*, 2018). The incorporation of limestone powder also benefits the mechanical properties by the filler and nucleating effect experienced under the alkaline environment; additionally, this is a widely abundant and low-cost material.
The use of MgO in combination with NaOH offers several advantages. MgO acts as a catalyst, accelerating the dissolution and polymerization reactions during the alkaline activation. It also promotes the formation of M-S-H gels, which improves the mechanical properties (Juan et al. 2021; Jiang et al. 2023). On the other hand, the NaOH is a strong alkaline activator enhancing the reactivity of diverse SCMs.
The utilization of NaOH and MgO activators in cementitious materials represents a pivotal aspect of sustainable construction practices. While both activators contribute to the alkaline activation process, it is imperative to evaluate their suitability from a sustainability standpoint. In certain geographic regions, the production of MgO may entail a lower environmental impact compared to NaOH, thereby offering a potential advantage in terms of sustainability (Mendes et al.2021;

Hongqiang et al. 2023). This consideration underscores the importance of assessing and discussing the environmental implications associated with the choice of activators in alkaline activation processes.

Despite the potential benefits of the alkaline activation, the optimization of the activation process and the characterization of the resulting materials remain as a key challenge. The properties of the activated cements are influenced by various factors, including the composition of the blend, the MgO/NaOH ratio, the curing conditions and the activator concentration. Understanding the complex interactions between these factors is essential for tailoring the properties of the activated cements to meet specific performance requirements. Therefore, this study aims to investigate the effects of MgO-NaOH blends as alkaline activators on the compressive strength evolution and microstructure of blended limestone powder and fly ash cements, by systematically varying the activation parameters and characterizing the resulting materials. All the result were supported on the use of XRD, SEM and thermal analysis which enables a detailed examination of the microstructure and phase composition of alkali activated pastes, providing insights into its performance at later ages of curing. The main goal is to understand the involved mechanisms governing the alkaline activation process and its impact on the performance of the activated limestone-CV cements up to 360 days of curing. The findings contribute to the development of sustainable cementitious materials that incorporate high quantities of low cost and available materials.

2. EXPERIMENTAL PROCEDURE

2.1 Materials

For the preparation of the alkali-activated pastes, commercial limestone and Class C-CV were used as the main solid precursors. Table 1 shows the chemical composition determined by X-ray fluorescence for both raw materials. It can be observed that limestone powder (PClz) is mainly composed of CaO in the form of calcite with a density of 2.8 g/cm^3 (measured according to ASTM C 188-17, 2017) and a surface area of 450 m^2/kg determined by the air permeability test (ASTM C204 – 11, 2011). On the other hand, the CV contained SiO_2 and Al_2O_3 with a surface area of 525 m^2/kg and minor amounts of MgO which are expected to be contained in the glassy phase of the by-product. The limestone sand with a particle size <4mm underwent a grinding process of 25 min in a ball mill, in order to reduce the particle size of the material to improve its reactivity, whereas the Class C fly ash was used as received.

Table 1. Oxide composition (as per X-ray fluorescence) and physical properties of solid precursors

	Oxide (expressed in wt%)										Density, (kg/m^3)	LOI*	Surface area, m^2/kg
	CaO	SiO_2	Al_2O_3	MgO	SO_3	TiO_2	K_2O	Fe_2O_3	MnO	Na_2O			
PClz	56.84	1.052	---	0.28	---	---	0.63	0.054	--	0.052	2.8	41	450
CV	19.4	42.23	23.03	3.47	2.02	1.24	0	4.42	--	--	---	0.06	525

*LOI= Loss on ignition

Figure 1 a) shows the X-ray diffraction patterns of the limestone powder and CV. Crystalline phases of calcite were observed for limestone with different intensities, with one of the most prominent peaks appearing around 29° 2θ. In contrast, fly ash displayed an amorphous hump between 20-40° 2θ, which was directly related to the amorphous phase present in the material. It has been reported that the amorphous phase is related to the reactivity of the material under alkaline conditions to further form cementitious phases. Therefore, it could be anticipated that the contact of the CV with an alkaline solution will promote the breaking of the atomic structure to form

cementitious phases (Guanqi et al. 2023). Some additional crystalline phases detected were quartz, mullite, and hematite (Vivek et al. 2019) as can be seen in Figure. (a). On the other hand, Figure (b) shows information about the particle size distribution for both raw materials. It is noted that CV has a d50=10.9 µm while limestone is coarser with a d50=17.9 µm. Limestone showed an irregular morphology of particles while CV exhibited a typical spherical morphology as it is observed in Figures (c) and (d) respectively. MgO powder and pellets of NaOH reagent degree were incorporated as chemical activators. The reactivity of the MgO was of 32 s measured by the acid acetic test described by (Shand. 2006).

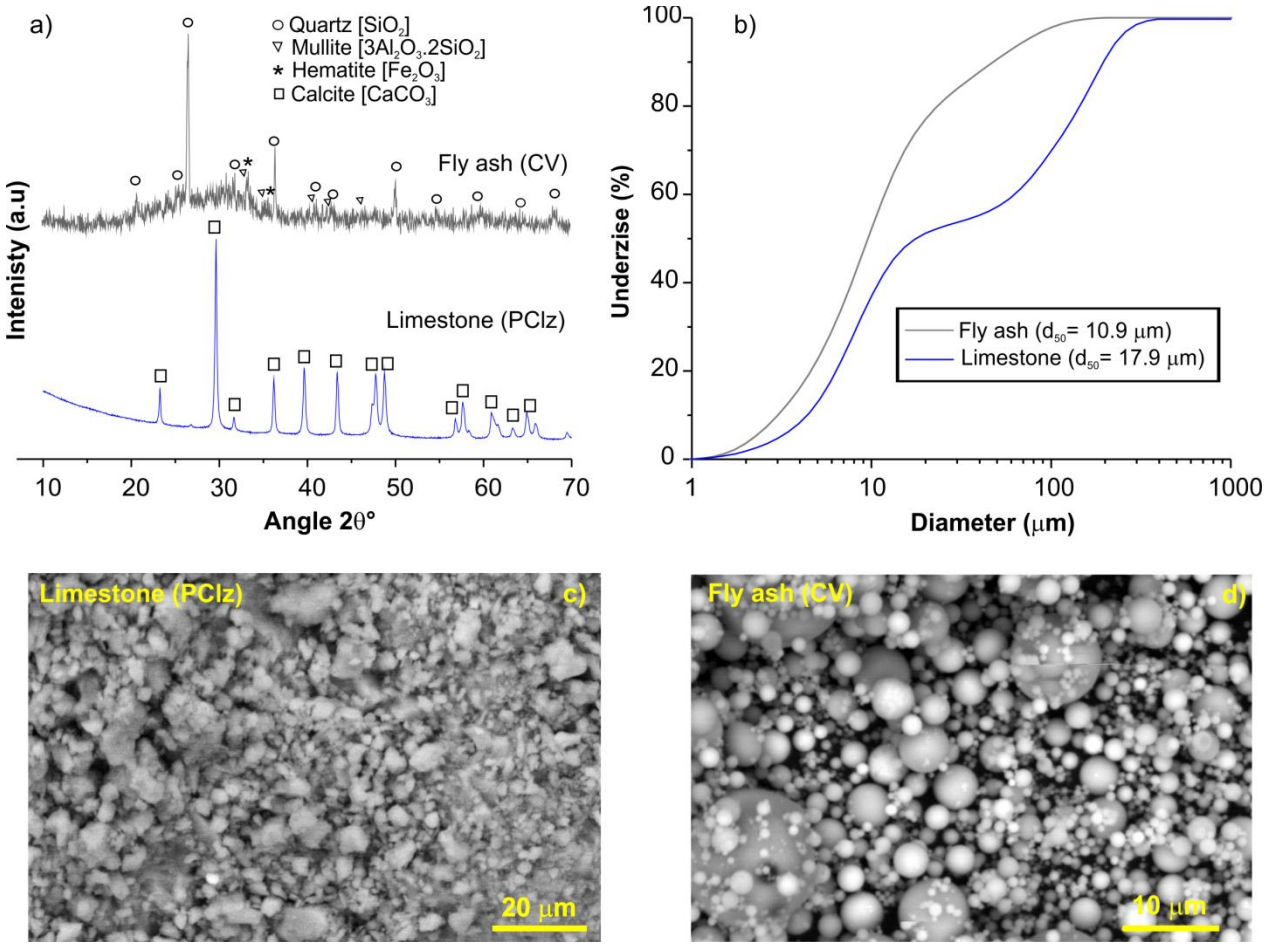

Figure 1. X-ray diffraction patterns of limestone and class C fly ash (CV) a), particle size distribution of both materlas (Burciaga-Díaz et al. 2023), limestone morphology c) and fly ash morphology d).

2.2 Sample preparation

For the chemical activation of the raw materials, a blend of MgO:NaOH at a 1:1 ratio was utilized as the activating agent, accompanied by water to dissolve the solid precursors, at a ratio of water to binder = 0.25 relative to the mass of the binder (PClz + CV). The mixtures were cured at 40°C for 24 hours, followed by subsequent curing at 20°C for up to 360 days. The concentrations of the alkaline activator used are presented in Table 2. Nine formulations of pastes were assessed, varying the ratios of PClz/CV from 100/0, 75/25, 50/50, 25/75, to 0/100. The pastes were activated with 8%, 10%, 12%, 14%, and 16% of MgO-NaOH (1:1 ratio) and represented by the nomenclature MO-NH in the ID line. Samples of references corresponding to the pastes with 100 % CV (MO-NH-0-12) and 100% PClz (MO-NH-100-12) were used to compare the performance of the alkali activated formulations incorporating different amount of PClz/CV.

Table 2. Composition of the formulated pastes.

ID	PClz (wt.%)	CV (wt. %)	Blended Activators at ratio 1:1 (wt. %)
MO-NH-25-10	25	75	10
MO-NH-25-14	25	75	14
MO-NH-75-10	75	25	10
MO-NH-75-14	75	25	14
MO-NH-50-8	50	50	8
MO-NH-50-16	50	50	16
MO-NH-0-12	0	100	12
MO-NH-100-12	100	0	12
MO-NH-50-12	50	50	12

The alkaline solutions were prepared by dissolving MgO and NaOH in water in appropriate proportions for each formulation. Subsequently, the pastes were prepared by adding the solid powder precursors to the previously prepared solution with constant stirring for 3 minutes. The fresh pastes were poured into 2.5 cm cubic molds. The pastes were vibrated for 20 seconds to remove trapped air, and the molds were covered with wet cloth and plastic to prevent moisture losses. The alkali activated cements were then placed in an isothermal chamber at 40°C. After 24 hours, the cubic samples were demolded and stored in plastic bags, continuing with their curing for up to 360 days at 20°C.

After 1, 7, 14, 28, 90, 180, and 360 days, a hydraulic press machine with a constant load rate of 300 N/s was used to measure the compressive strength of 4 randomly selected cubes, reporting the average value. After the tests, solid fragments were collected and immersed in acetone. After 24 hours, the acetone was removed and the collected fragments were oven dried for 2 days at 40°C to stop hydration reactions. Several articles in the literature have reported the interruption of cement hydration when exposed to organic solvents such as acetone, which has proven to be effective. However, it is worth mentioning that solvents can induce physical interactions with the hydrates, resulting in microstructural contractions and potential condensation of secondary products. Nevertheless, the available characterization techniques do not provide sufficient information about the by-products that could hinder adequate interpretation (Zhang and Scherer. 2021).

2.3 Caracterization

The collected fragments were manually pulverized in an agate mortar and sieved through a #140 mesh for subsequent characterization by X-ray diffraction (XRD) (PANalytical, Empyrean) in a range of 10°-80° (2θ) with a step speed of 0.03°/s using CuKα radiation.

For thermogravimetric analysis, a simultaneous thermal analyzer ATG/ADT SDT Q-600 with an alumina crucible was used, with a heating rate of 10°C/min up to 900°C to evaluate mass changes and exothermic and endothermic events associated with decomposition and formation of reaction products.

Selected samples were mounted in epoxy resin, polished, and analyzed under a scanning electron microscope (SEM) (JEOL JSM-6610 LV) with energy-dispersive spectroscopy (EDS) attachment (Oxford Instruments X-max) of 20 mm². Images were obtained from representative areas in backscattered electron (BSE) mode at 500x magnification with a 20 kV current in high vacuum mode.

3. RESULTS

3.1 Compressive strength

Figure 1 shows the compressive strength (CS) results for the PClz-CV alkali activated cements as solid precursors, based on the amount of limestone and % of MgO-NaOH, up to 360 days of curing. For most systems, an increase in CS was observed from the first day of curing, suggesting that the combination of alkaline agents promoted an effective dissolution of reactive species and the condensation of reaction products with good mechanical properties. However, the system containing 100% limestone (MO-100-12) did not show any increase in strength at any curing date, suggesting that the activation conditions for this system did not favor the dissolution of limestone and the formation of cementitious products.

The graph shows that as the presence of PClz in the formulation increased, from 25% to 50%, the mechanical properties decreased, even for additions up to 75% (MO-NH-75-10, MO-NH-75-14). it has been reported that additions of PClz of 30% promoted effective strength gains in Portland cement systems, due to the Ca^{2+} released from the limestone participating in hydration reactions and by its filling effect according to Gao et al. (2015).

Additionally, the MO-NH-25-10 (with 25%PClz-75%CV) binder developed the highest CS of 76 MPa after 360 days of curing. Furthermore, the formulations containing 50% PClz-50%CV with 8 and 16 % of activator achieved CS levels between 7.4-11.7 MPa and 48.3-49.2 MPa at 1 and 360 days of curing, respectively, which is interesting considering the high amount of PClz (50%) present in the formulations. It is important to highlight that the MO-NH-50-12 binder was elaborated twice to confirm the reproducibility of the experimentation. The compressive strength remained very similar up to 360 days, with a standard deviation of about 5 MPa, demonstrating good reproducibility of the results. The positive trend in compressive strength development indicated that the use of MgO combined with NaOH in the activator favored the formation of stable cements, even up to 360 days of curing (Ávila-López et al., 2015). The results are interesting, considering that most reports in the literature typically focus on properties assessed within curing periods of up to 28 days. Further studies evaluating properties over longer durations (i.e., up to 360 days) as proposed in this research are necessary to gain a better understanding of the effects of PClz and mixtures of NaOH-MgO on the stability of alkali-activated cements (Wang, D., et al. 2020; Wang, Z., et al. 2021). In this regard, the assessed samples demonstrated dimensional stability despite the presence of MgO, which is known to potentially form expansive phases such as brucite ($Mg(OH)_2$) in Portland cement-based binders, suggesting its significant role in forming stable reaction products.

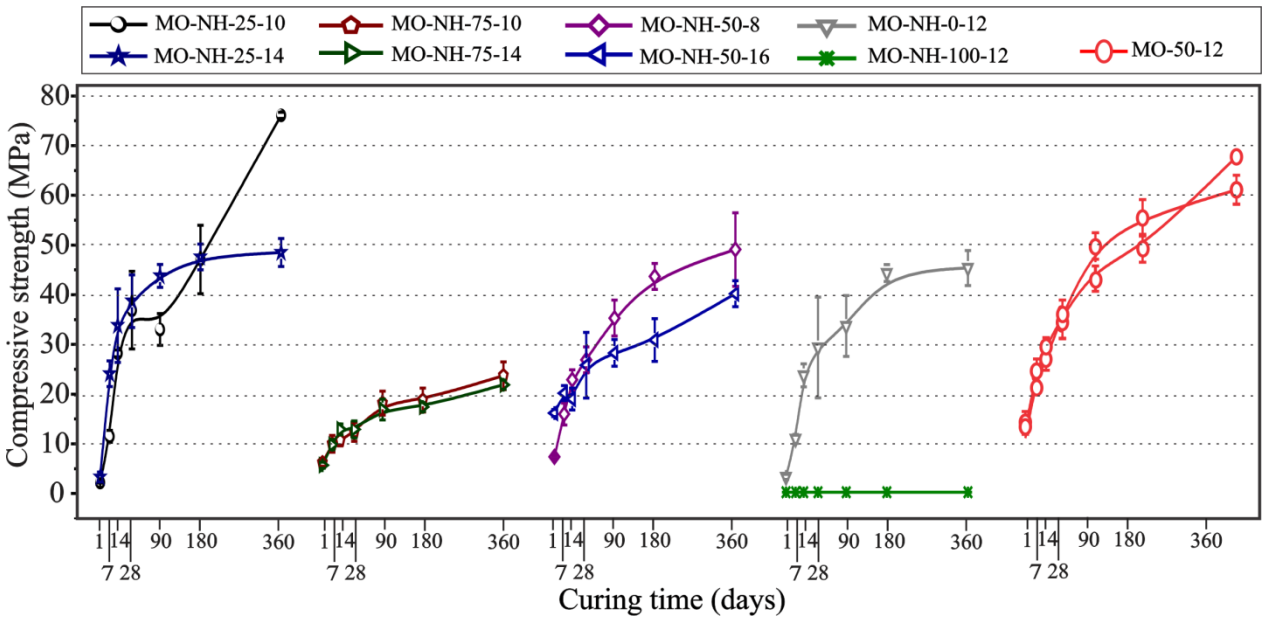

Figure 1. Compressive strength vs time for pastes activated with MgO-NaOH up to 360 days of curing.

3.2 X-ray diffraction (XRD)

Figure 2 shows the XRD patterns of the MO-0-12, MO-25-10, and MO-50-12 pastes, at 28 and 180 days of curing, with the patterns of unreacted limestone and fly ash included for reference. The analyzed pastes were chosen based on the highest levels of compressive strength observed at 360 days.

After the chemical activation process of the solid precursors, the patterns did not experience important differences in comparison with the starting precursors (PClz and fly ash). The calcite reflections remained and an amorphous hump between 25-35° 2θ was observed from 28 days of curing onwards, which was associated with the vitreous phase of the fly ash and possible formation of disordered reaction products such as calcium silicate hydrate (C-S-H) with Na and Al incorporation in its structure. In alkali-activated cements, the C-S-H ($5CaO{\cdot}3SiO_2{\cdot}2H_2O$) is reported at 29.4° 2θ ($CaCO_3$, PDF # 01-086-2340), which makes its detection complicated by its illcrystalline/amorphous nature and by the overlapping with calcite peaks ($CaCO_3$) (Mobasher et al. 2016). However, according to the compressive strength results at both curing dates, this phase could be formed, as it is the main binding phase responsible for the mechanical properties in alkali-activated cements, as reported by Taewan Kim and Yubin Jun (2018).

When the amount of PClz increased to 50% in the alkali activated cements, the intensity of the amorphous hump decreased by a dissolution effect caused by the limestone addition in which the amount of crystalline calcite attenuated the amorphous products as can be seen in paste MO-50-12 compared with MO-0-12 and MO-25-10.

Minor reflections of gaylussite [($Na_2Ca(CO_3)_2.5H_2O$; PDF # 002-0122] and pirssonite [$Na_2Ca(CO_3)_2{\cdot}2H_2O$; PDF # 24-1065] were also detected in all pastes which formed due to the partial dissolution of calcite with the chemical activators (Ortega-Zavala et al. 2019; Firdous et al. 2021). In addition, some low-intensity crystalline reflections of hydrotalcite [$Mg_6Al_2(CO_3)(OH)16{\cdot}4H_2O$; PDF # 014-0191] were detected in all the diffraction patterns. Fei Jin et al. (2015) reported that this phase fills the pores of the microstructure and increases the mechanical properties, which may have also contributed to the compressive strength values obtained at different curing dates; hydrotalcite is commonly reported in alkali activated binders containing Mg in its composition (Shade et al. 2022). Lastly, reflections of quartz were identified, which may be present in the raw material and act as inert filler.

.

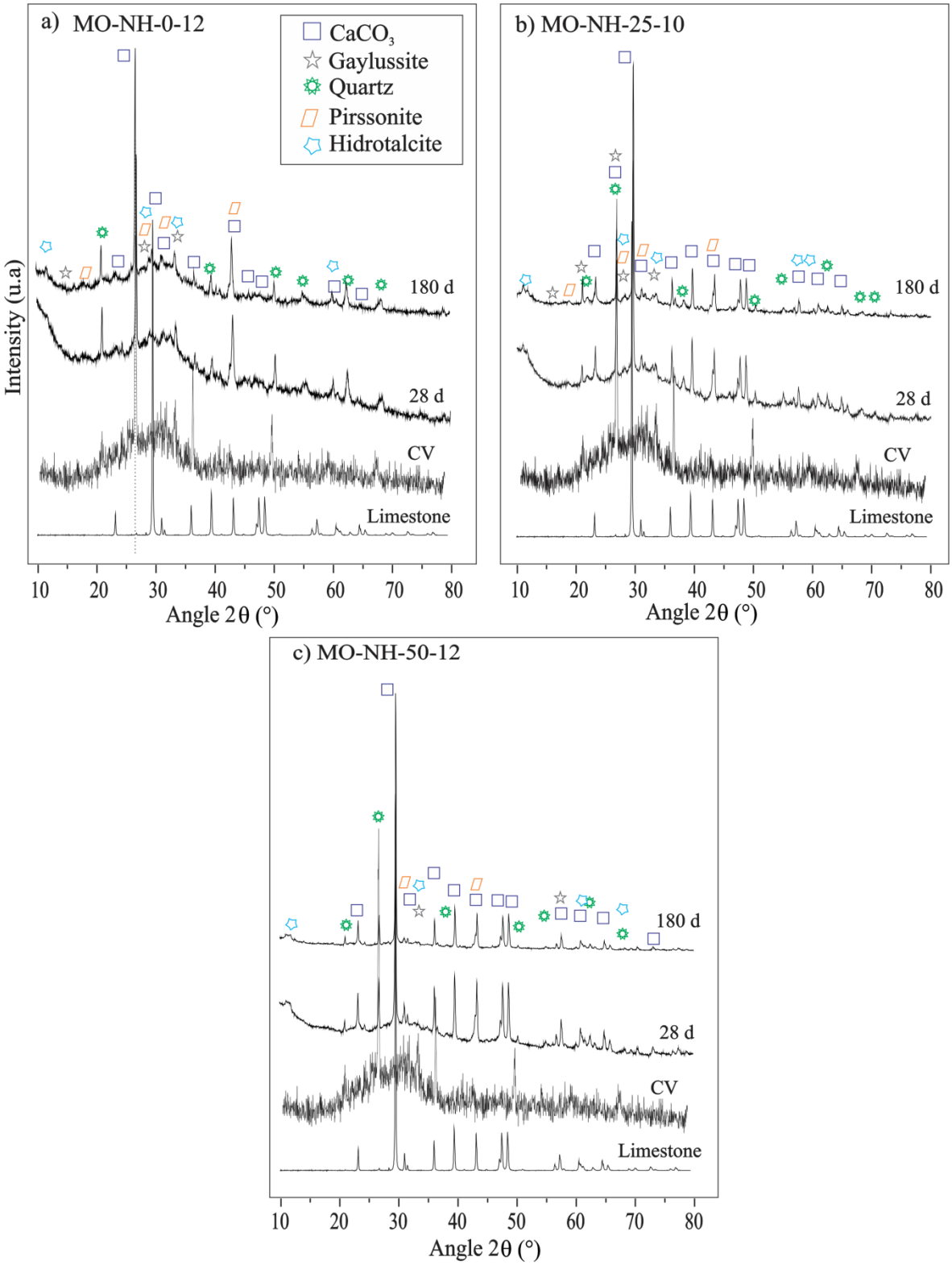

Figure 2. XRD patterns for different pastes MO-0-12 (a), MO-25-10 (b) and MO-50-12 at 28 and 180 days of curing.

3.3 Thermal analysis

Figure 3 shows results of thermogravimetric analysis for the alkali-activated limestone and fly ash systems at 28 and 180 days of curing, in terms of weight loss and its derivative. For both curing dates and for all systems, diverse weight losses corresponding to endothermic events were observed. Up to 200°C, the progressive dehydration of products such as C-S-H (calcium silicate hydrate) occurred. This is the main phase responsible for the gain of mechanical properties in hydrated cements. Additionally, the decomposition of hydrated phases such as Mg-(A)-S-H intermixed with C-S-H may occur.

In the pastes containing more than 25%PClz, the decomposition of pirssonite and gaylussite was also observed. The presence of these phases indicated that, during hydration reactions and over time, limestone partially dissolved, releasing Ca^{2+} and CO_3^{-2} ions that favored the formation of the mentioned carbonates (pirssonite and gaylussite) in addition to C-S-H, in agreement to Wang. D et al. 2018.

As the temperature increased to 400°C, the decomposition of hydrotalcite, also known as Mg-Al double-layer hydroxides, occurred. O. Burciaga-Díaz et al. (2018) reported similar weight losses between 550-600°C in alkali activated slag cements of blast furnace slag activated with a mixture of 4-8% MgO-NaOH, which were related to the dehydroxylation of hydroxyl groups (Mg-OH) attached to Mg^{2+} ions present in hydrated magnesium silicate (M-S-H) phases formed by the interaction of added MgO with the reactive silica from the amorphous structure of the CV in the alkaline environment. The presence of MgO detected previously in the chemical analysis in the unreacted CV was anticipated to be encapsulated within the glassy phase of the precursor, as indicated by the absence of any discernible crystalline phase in the X-ray diffraction (XRD) analysis. Rather than functioning solely as an activator, MgO is regarded more as an additive in this context. When combined with NaOH, MgO exerts a synergistic effect, facilitating the formation of key cementitious phases such as M-S-H (Magnesium Silicate Hydrate) and hydrotalcite. These phases contribute significantly to the mechanical strength and durability of the alkali-activated cements, enhancing their overall performance characteristics (Xinyuan et al. 2017).

Around 750°C, the detected endothermic peak was related to the decomposition of $CaCO_3$ present in the unreacted PClz used as a cementitious precursor (limestone) based on the following reaction $CaCO_3 \rightarrow CaO + CO_2$ (Karunadasa et al., 2019). At 180 days of curing, the thermograms did not show significant changes, but the mass losses were higher in the range of 50-250°C compared to those at 28 days. This suggests that an increased formation of hydration reactions such as C,N-A-S-H occurred considering the positive evolution of the compressive strength at later curing ages.

Apparently, the PClz-CV ratio influenced the M-S-H formation as can be seen in samples MO-NH-25-10 and MO-NH-50-12 contrary to the paste MO-NH-0-12, which did not display its formation. All the discussed phases were better observed in the derivative curves, which showed well-defined endothermic peaks corresponding to the decomposition stages of the precipitated products.

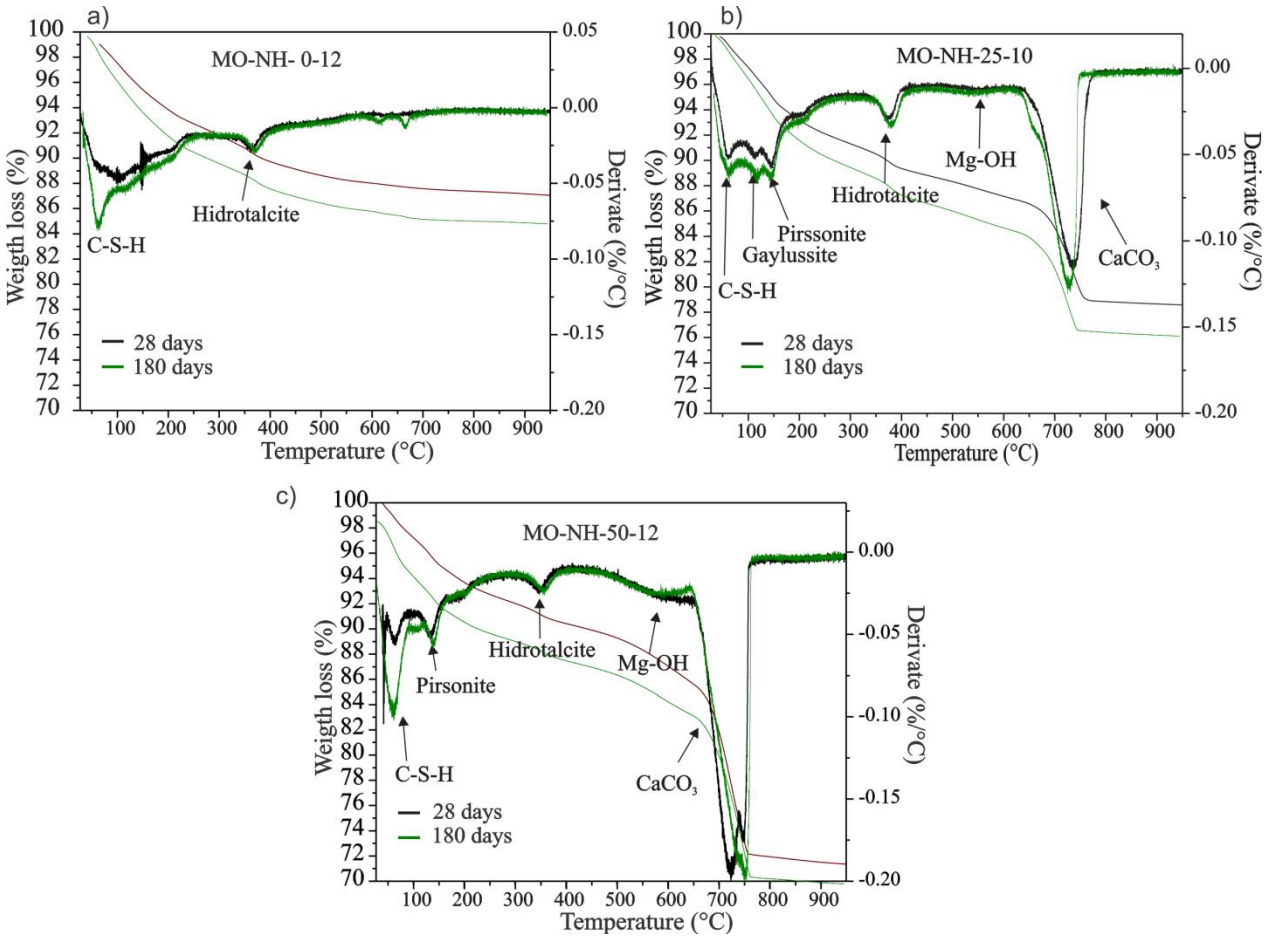

Figure 3. Thermogravimetric analysis curves and their derivative for pastes MO-0-12 (a), MO-25-10 (B) and MO-50-12 (C) at 28 and 180 days.

3.4 Scanning electron microscopy (SEM)

Figure 4 shows backscattered electron microstructures at 28 days of curing for MO-0-12, MO-25-10, and MO-50-12 pastes. The analyzed pastes were considered based on its high compressive strength. In general, limestone particles could be observed and distinguished by their irregular and smooth morphology, while CV particles had spherical morphology and light gray tone, found partially and fully reacted. In paste MO-NH-0-10, the microstructure was formed by unreacted CV particles homogenously dispersed in a matrix of reaction products of dark gray tone. Around some CV particles reaction rims were identified corresponding to precipitated cementitious phases produced by the interaction of fly ash with the MgO- NaOH alkaline solution especially in pastes MO-NH-25-10 and MO-NH-50-12. The low porosity observed in the different pastes was consistent with the observed compressive strength values at 28 days, which exceeded 29 MPa. With PClz above 25% in substitution of CV, the microstructure was more densified, suggesting that the activation conditions favored the dissolution of reactive species and the formation of reaction products that improved the compressive strength. A previous study (Kalinkin et al. 2020) linked the presence of PClz in fly ash pastes with a more intensive and accelerated reaction than t in absence of PClz suggesting the acceleration of the geopolymerization process by the active participation of $CaCO_3$ as nucleation sites in agreement with the observed densification of the microstructures. On the other hand, for the MO-50-12 formulation, a dense interphase was observed between the limestone frontiers and the reaction product matrix, allowing its compressive strength to be among the highest values obtained within these formulations.

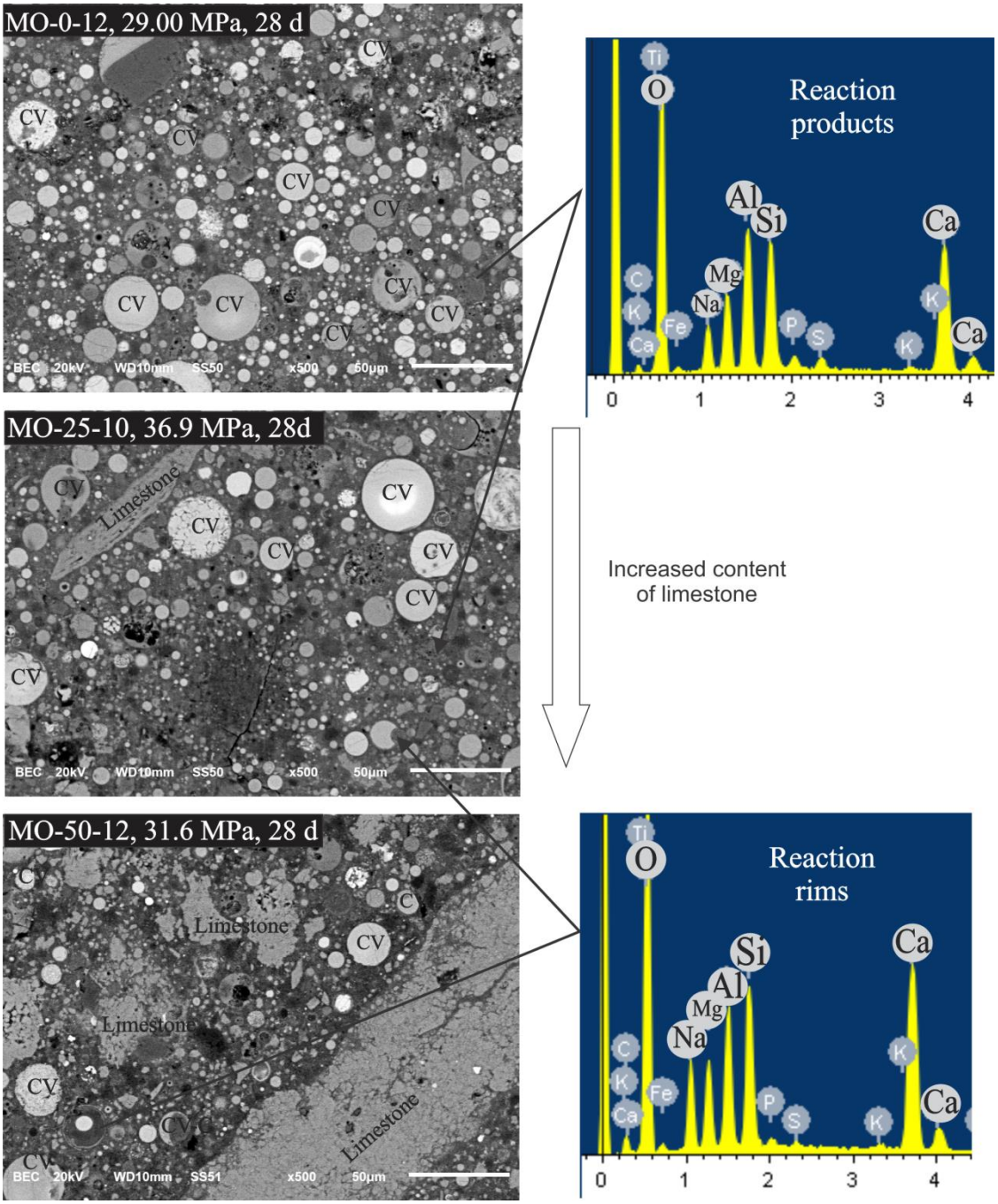

Figure 4. Scanning electron micrographs of samples pastes MO-0-12, MO-25-10 and MO-50-12 at 28 days.

The relatively high amount of unreacted limestone in the paste MO-50-12 could have acted as filler, reinforcing the microstructures. This effect occurred when limestone filled available spaces between particles, densifying the microstructures, as reported previously by Li et al. (2020). However, it is possible that PClz could have partially participated in the hydration processes by forming C, N-A-S-H, acting as a nucleation agent, in agreement with Xiang et al. (2018). The energy dispersive spectroscopy results confirmed the formation of reaction products with a high concentration of Al, Si, Ca, Mg, and Na, in agreement with the precipitation of C,N-A-S-H type gels (Walkley et al., 2016). Reaction rims around the CV particles showed higher concentrations of Ca than the reaction products, indicating differences in the chemical composition of the

precipitated phases.
Finally, unreacted MgO particles were not identified, indicating its effective participation in the chemical reactions and incorporation into the products to form M-S-H type gels and hydrotalcite phases (Bernard et al. 2017; Lauermannová et al. 2020), as discussed previously.

4. CONCLUSIONS

According to the compressive strength results, the utilization of the MgO-NaOH mixture facilitated the effective dissolution of the limestone and fly ash blend. Notably, samples featuring 50%PClz-50%CV and 25%PClz-75%CV, with 12% and 10% NaOH-MgO respectively, exhibited compressive strengths of 69 and 76 MPa, respectively suggesting the active involvement of both CV and limestone in the hydration reactions. XRD and Thermal analysis results indicated the partial dissolution of PClz under alkaline conditions, leading to the formation of carbonated phases, while CV emerged as the most reactive material contributing to strength gain.
Observations from SEM at later stages revealed that PClz enhanced strength through a filler effect, resulting in a microstructure densification. However, concentrations of PClz exceeding 75% led to a substantial reduction in the compressive strength due to dilution effects. SEM and EDS analysis suggested the formation of low-porosity microstructures characterized by high concentrations of Si, Al, Ca, Mg, and Na, associated with the formation of C-S-H (with Al and Na uptake), M-S-H, gaylussite, pirssonite, and hydrotalcite.
Furthermore, the presence of MgO as an additive did not exhibit detrimental effects on the alkali-activated pastes within the 360-day curing period. These findings underscore the potential of limestone to be utilized as a substitute for CV. Overall, this study presents original insights and can serve as basis for formulating other alkali-activated cements incorporating limestone in combination with other more reactive precursors.

5. ACKNOWLEDGEMENTS

I.E. Betancourt Castillo thanks CONACYT for the doctoral scholarship 711629 granted to pursue graduate studies at TecNM campus Saltillo. The authors also thank the financial support granted by the Tecnológico Nacional de México project 5609.15 and the facilities provided by the Instituto Tecnológico de Saltillo for the development of the research.

6. REFERENCES

Villágran-Zaccardi, Y., Pareja, R., Rojas, L., Irassar, E., Torres-Acosta, A., Tobón, J., Jhon. V. M. (2022). *Overview of cement and concrete production in Latin America and the Caribbean with a focus on the goals of reaching carbon neutrality.* RILEM Technical Letters, 7: 30-46.
Alsalman, A., Assi, L. N., Kareem, R. S., Carter, K., Ziehl, P. (2021). *Energy and CO2 emission assessments of alkali-activated concrete and Ordinary Portland Cement concrete: A comparative analysis of different grades of concrete,* Cleaner Environmental Systems, 3, 100047, https://doi.org/10.1016/j.cesys.2021.100047.
Mendoza-Rangel, J. M., Díaz-Aguilera, J. H. (2023). *Circular economy in the Latin American cement and concrete industry: a sustainable solution of design, durability, materials, and processes.* Revista ALCONPAT, 13(3), 328 - 348. https://doi.org/10.21041/ra.v13i3.697
Mohamed, O. A., Najm, O., Ahmed, E. (2023) *Alkali-activated slag & fly ash as sustainable alternatives to OPC: Sorptivity and strength development characteristics of mortar,* Cleaner Materials, 8, 100188, https://doi.org/10.1016/j.clema.2023.100188.

Juenger, M. C. G., Snellings, R., Bernal, S. A. (2019), *Supplementary cementitious materials: New sources, characterization, and performance insights,* Cement and Concrete Research, 122, 257-273, https://doi.org/10.1016/j.cemconres.2019.05.008.

Temuujin, J., Surenjav, E., Ruescher, C. H., Vahlbruch, J. (2019), *Processing and uses of fly ash addressing radioactivity (critical review),* Chemosphere, 216, 866-882, https://doi.org/10.1016/j.chemosphere.2018.10.112.

Chan, C. L., Zhang, M. (2023), *Effect of limestone on engineering properties of alkali-activated concrete: A review,* Construction and Building Materials, 362, 129709, https://doi.org/10.1016/j.conbuildmat.2022.129709.

Ortega-Zavala, D. E., Santana- Carrillo, J. L., Burciaga Díaz, O. Escalante-García. J. I. (2019). *An initial study on alkali activated limestone binders.* Cement and Concrete Research. 120, 267-278. https://doi.org/10.1016/j.cemconres.2019.04.002

Dehui Wang, Caijun Shi, Nima Farzadnia, Zhenguo Shi, Huangfei Jia, Zhihua Ou. (2018). *A review on use of limestone powder in cement-based materials: Mechanism, hydration and microstuctures*. Construction and Building Materials. 181, 659-672. https://doi.org/10.1016/j.conbuildmat.2018.06.075

Fei Jin, Kai Gu, Adel Abdollahzadeh, and Abir Al-Tabbaa (2015). *Effects of different reactive MgOs on the hydration of MgO-Activated GGBS paste.* J. Mater. Civ. 27. https://doi.org/10.1061/(ASCE)MT.1943-5533.0001009

Saleh, H. M., Eskander, S. B. (2020). *18 – Innovative cement-based materials for environmental protection and restoration, in: Samui Pijush, Kim, Dookie, R. Iyer Nagesh, Chaudhary Sandeep* (Eds.), New Materials in Civil Engineering, Butterworth-Heinemann, pp. 613-641. https://doi.org/10.1111/j.1151-2916.2003.tb03623.x

Díaz-Aguilera, J. H. (2024). *Estudio del diseño eficiente, optimización, durabilidad y sostenibilidad de una pasta de mortero activado alcalinamente con base en metacaolin y piedra caliza.* Doctorado thesis, Universidad Autonóma de Nuevo León. http://eprints.uanl.mx/id/eprint/27180

Xiang, J., Liu,l., Cui, X., He, Y., Zheng, G., Shi, C. (2018). *Effect of limestone on rheological, shrinkage and mechanical properties of alkali – Activated slag/fly ash grouting materials.* Construction and Building Materials. 191, 1285-1292. https://doi.org/10.1016/j.conbuildmat.2018.09.209

Burciaga-Díaz, O., Betancourt-Castillo, I. E. (2018). *Characterization of novel blast-furnace slag cement pastes and mortars activated with a reactive mixture of MgO-NaOH*. Cement and Concrete Research. 105, 54-63. https://doi.org/10.1016/j.cemconres.2018.01.002

Kalinkin, A. M., Gurevich, B. I., Myshenkov. M. S. Chislov, M. V., Kalinkina, E. V., Zvereva. I. A., Cherkezova-Zheleva, Z., Paneva, D., Petkova. V. (2020). *Synthesis of Fly Ash-Based Geopolymers: Effect of Calcite Addition and Mechanical Activation.* Minerals. 10(9):827. https://doi.org/10.3390/min10090827

Juan, H., Weihao, Z., Wenbin, B., Tingting, H., Junhong, H., Xuefeng, S. (2021). *Effect of reactive MgO on hydration and properties of alkali-activated slag pastes with different activators*, Construction and Building Materials, 271, 121608, https://doi.org/10.1016/j.conbuildmat.2020.121608

Jiang, Y., Jia, Y., Zou, X., Zhang, J., Zou, Y. (2023). *Evolution mechanism of the low-carbon MgO-based alkali-activated system under different heat-treatment conditions.* Materials Science and Technology, *39*(18), 3220–3228. https://doi.org/10.1080/02670836.2023.2245659.

Mendes, B. C., Pedroti, L. G., Maurício, C., Vieira, F., Marvila, M., Azevedo, A. R. G. Franco de Carvalho, J. F., Ribeiro. J. C. L. (2021) *Application of eco-friendly alternative activators in alkali-activated materials: A review*, Journal of Building Engineering, 35, 2021, 102010, https://doi.org/10.1016/j.jobe.2020.102010.

Hongqiang, M., Xiaomeng L., Xuan, Z., Xiaoyan N., Youliang F. (2022) *Effect of active MgO on the hydration kinetics characteristics and microstructures of alkali-activated fly ash-slag materials,* Construction and Building Materials, 361, 129677, https://doi.org/10.1016/j.conbuildmat.2022.129677.

ASTM C188-17. (2017). *Standard Test Method for Density of Hydraulic Cement,* ASTM international, West Conshohocken, PA.

ASTM C204 – 11. (2011). *Standard Test Methods for Fineness of Hydraulic Cement by Air-Permeability Apparatus*. ASTM international, West Conshohocken, PA.

Guanqi, W., Biqin, D., Guohao, F., Yanshuai W. (2023). *Understanding reactive amorphous phases of fly ash through the acidolysis*, Cement and Concrete Composites, 140, 105102, https://doi.org/10.1016/j.cemconcomp.2023.105102.

Vivek, G., Salman, S., Sandeep, C. (2019) *Characterization of different types of fly ash collected from various sources in Central India*, Materials Today: Proceedings, 18, Part 7, 5076-5080, https://doi.org/10.1016/j.matpr.2019.07.503.

Shand, M. A. (2006). The Chemistry and Technology of Magnesia, Wiley, Hoboken, NJ, USA.

Zhang, Z., Scherer, G. W. (2021), *Physical and chemical effects of isopropanol exchange in cement-based materials*, Cement and Concrete Research, 145, 106461, https://doi.org/10.1016/j.cemconres.2021.106461.

Wang. D, Gao, X., Wang, R., Larsson, S., Benzerzour, M. (2020). *Elevated curing temperature-associated strength and mechanisms of reactive MgO-activated industrial by-products solidified soils.* Marine Georesources & Geotechnology, 38(6), 659–671. https://doi.org/10.1080/1064119X.2019.1610817

Xinyuan K, Bernal, S. A., Provis, J. L. (2017). *Uptake of chloride and carbonate by Mg-Al and Ca-Al layered double hydroxides in simulated pore solutions of alkali-activated slag cement,* Cement and Concrete Research, 100, 1-13, https://doi.org/10.1016/j.cemconres.2017.05.015.

Karunadasa, K. S. P., Manoratne, C. H., Pitawala,H.M., Rajapakse, R.M.G. (2019). *Thermal decomposition of calcium carbonate (calcite polymorph) as examined by in-situ high temperature X-ray powder diffraction*, Journal of Physics and Chemistry of Solids,134, 21-28. https://doi.org/10.1016/j.jpcs.2019.05.023.
(https://www.sciencedirect.com/science/article/pii/S0022369719301970)

Wang, Z., Park, S., Khalid, H. R., Lee, H. K. (2021) *Hydration properties of alkali-activated fly ash/slag binders modified by MgO with different reactivity,* Journal of Building Engineering, 44, 103252. https://doi.org/10.1016/j.jobe.2021.103252.

Firdous, R., Hirsch, T., Klimm, D., Lothenbach, B., Stephan, D. (2021). *Reaction of calcium carbonate minerals in sodium silicate solutions and its role in alkali-activated systems.* Minerals Engineering. 165, 106849. https://doi.org/10.1016/j.mineng.2021.106849.

Schade, T., Bellmann, F., Middendorf, B. (2022). *Quantitative analysis of C-(K)-A-S-H-amount and hydrotalcite phase content in finely ground highly alkali-activated slag/silica fume blended cementitious material*, Cement and Concrete Research, 153, 2022, 106706, https://doi.org/10.1016/j.cemconres.2021.106706.

Burciaga-Díaz, O., Betancourt-Castillo, I. E., Escalante-García, J. I. (2023). *Limestone and class C fly ash blends activated with binary alkalis of Na_2CO_3-NaOH and MgO-NaOH: Reaction products and environmental impact.* Cement and Concrete Composites, 137, 104949. https://doi.org/10.1016/j.cemconcomp.2023.104949

Andrew, R. M. (2019), *Global CO_2 emissions from cement production,* Earth Science Data (1928-2018), http://doi.org/10.5194/essd-2019-152.

Mobasher, N., Bernal, S. A., Provis, J. L. (2016) *Structural evolution of an alkali sulfate activated slag cement,* Journal of Nuclear Materials, Volume 468, 97-104. https://doi.org/10.1016/j.jnucmat.2015.11.016.

Li, C. H., Jiang, L. (2020). *Utilization of limestone powder as an activator for early-age strength improvement of slag concrete,* Construct. Build. Mater. 253, 119257. https://doi.org/10.1016/j.conbuildmat.2020.119257.

Lauermannová, A-M., Paterová, I., Patera J., Skrbek, K., Jankovský, O., Bartůněk, V. (2020) *Hydrotalcites in Construction Materials.* Applied Sciences. 10(22):7989. https://doi.org/10.3390/app10227989

Walkley, B., San Nicolas, R., Sani, M. A., Rees, G. R., Hanna, J. V., van Deventer, J. S. J., John L. Provis, J. L. (2016). *Phase evolution of C-(N)-A-S-H/N-A-S-H gel blends investigated via alkali-activation of synthetic calcium aluminosilicate precursors,* Cement and Concrete Research, 89, 2016, 120-135, https://doi.org/10.1016/j.cemconres.2016.08.010.

Bernard, E., Lothenbach, B., Rentsch, D., Pochard, I., Dauzères, A. (2017). *Formation of magnesium silicate hydrates (M-S-H).* Physics and Chemistry of the Earth, Parts A/B/C, 99, 2017,142-157, https://doi.org/10.1016/j.pce.2017.02.005.

Taewan Kim and Yubin Jun. (2018). *Mechanical Properties of Na_2CO_3-Activated High-Volume GGBFS Cement Paste.* Advances in Civil Engineering. Vol. 2018, Article ID 8905194, 9 pages. https://doi.org/10.1155/2018/8905194

Ávila-López, U., Almanza-Robles,J.M., Escalante-García, J. I. (2015). *Investigation of novel waste glass and limestone binders using statistical methods.* Constr. Build Mater. 82, 296-303. https://doi.org/10.1016/j.conbuildmat.2015.02.085

Gao, X., Yu, Q. L., Brouwers. H. J. H. (2015). *Properties of alkali activated slag–fly ash blends with limestone addition.* Cement and Concrete Composites, 59, 119-128. https://doi.org/10.1016/j.cemconcomp.2015.01.007